FACTA UNIVERSITATIS
Series: **Electronics and Energetics** Vol. 32, N° 4, December 2019, pp. 615-631
https://doi.org/10.2298/FUEE1904615S

DEVELOPMENT OF AN AUTOMATED GAS-LEAKAGE MONITORING SYSTEM WITH FEEDBACK AND FEEDFORWARD CONTROL BY UTILIZING IOT

Mhia Md. Zaglul Shahadat, Avijit Mallik, Md. Monowarul Islam

Dept. of Mechanical Engineering, Rajshahi University of Engineering & Technology, Rajshahi, Bangladesh

Abstract. *Liquefied Petroleum Gas (LPG) is used in many ranges of applications like home and industrial appliances, in vehicles and as a propellant and refrigerator. However, leakage of LPG produces hazardous and toxic impact on human begins and other living creatures. There by, the authors developed a system to monitor the LPG gas leakage and make alert to users of it. In this research, MQ-6 gas sensor is used for sensing the level of gas concentration of a closed volume; and to monitor the consequences of environmental changes an IoT platform has been introduced. Robust control along with cloud based manual control has been applied so that the gas leakage can be prevented in the response of either feedback or feedforward commands individually. It switches on the specified relays to control the level of gas concentration in the time of leakage the excess gas in times of leakage. It rechecks the value again and again if it crosses 300 ppm it will setup a relay-based switching on control mechanism using Thingspeak cloud. The controller used here is Node-MCU v:1.0. This research provides design approach on both software and hardware. Hence an embedded system comprising of Relay switches, Embedded C++, Gas sensor, Temperature & Humidity sensor along with Internet of Things (IoT) is fabricated to meet the objectives of the current research.*

Key words: *Internet of Things, Smart System, Gas Leakage Control, Embedded System*

1. INTRODUCTION

LPG comprises of a blend of propane and butane which is profoundly combustible compound. It is an odorless gas, because of which Ethanoate oil is included as incredible odorant, with the goal that spillage can be effectively identified. There are other global benchmarks like EN589 [1], amyl Mercaptan, and Tetrahydrothiophene which are most regularly utilized as odorants. LPG is one of the substitute powers utilized nowadays. LPG is likewise utilized as a substitute fuel in vehicles because of taking off in the costs

Received May 1, 2019; received in revised form September 3, 2019
Corresponding author: Avijit Mallik
Dept. of Mechanical Engineering, Rajshahi University of Engineering & Technology, Rajshahi-6204, Bangladesh
(E-mail: avijitme13@gmail.com)

of oil and diesel. Some people have low sense of smell, may or may not respond on low concentration of gas leakage. In such a case, some high security systems have become an essence to prevent gas leakage accidents. Bhopal, Chernobyl, Okishima gas tragedy was an example of gas leakage accident in India, Russia and Japan [2, 3]. Accidents due to gas leakage are increasing day by day in recent times. Inherently, the researchers focused their attention on developing a smart system to monitor and avoid the gas leakage incidents [4]. Gas leakage detection is not only important but stopping leakage within smallest time interval is equally essential. The authors have designed and fabricated a system capable of sniffing LPG leakage on the basis of volumetric concentration (ppm) and takes immediate action to control the situation by the aid of Internet of Things (IoT).

For a long time, wireless technologies have been a real target of hackers due to the easiness of intercepting traffic and attacking without being noticed as some weaknesses in its security protocols [5]. Wireless Sensor Networking's (WSN) are also a big target due to the importance of the information it holds. For many wireless applications, the authentication system is relied on a Pre-Shared Key (PSK) which must be established before starting data communication between two or more devices. In Wireless HART (Highway Addressable Remote Transducer Protocol) communication, PSK holds a Join Key (JK) having an 'Intrinsic Security (IS)' [6]. Only when the JK is compromised, the security is overcome and plenty of attacks may take place frequently. As a prevention, this research includes IoT utilized WSN's having developed state-of-the-art algorithms capable of detecting possible node capturing attacks along with timing delay measure technique to predict specific node viable to security threats [7, 8]. Industries utilizing gas-piping (Process, Pharmaceuticals, Chemical and Fuel-fired Power Plants) are considered as a reference to apply the proposed gas leakage monitoring and control utilizing WSN (IoT enabled with wirelessHART) as per the experimental findings of the research undertaken. Table 1 shows some selected referred works on gas leakage/concentration detection and control in recent times.

The literatures stated above were mainly focused on sensing environmental changes (like gas concentration, relative humidity of soil and air), but all of those recent works lags in swift feedforward control along with the digital signal processing (DSP) analysis (i.e. data coherence, stability of wireless data logging, noise filtering and etc.). This paper involves like previous literatures where the authors have designed an automated LPG gas concentration monitoring system with both automatic and manual actuator(s) controlling from an IoT operated embedded platform. This research focuses on monitoring volumetric concentration (in parts per millions, ppm) of economic gaseous fuels like petroleum gases, liquid petroleum gas, carbon based toxic gases (high on carbon mono-oxide) etc., and to alert specific administrators/operators about the leakage through an IoT server (*Thingspeak*) provided with both automatic along with decision based actuator controlling to mitigate probable accidents from gas leakage. It also includes temperature and relative humidity sensing inside the control volume to check unstable sensory behavior as per the sensor datasheet.

Table 1 Referred works on electronic sensor-based gas concentration detection and actuator control.

Year	Purpose of research	Major findings	References
2014	Development of an Electronic nose for selected oil odor detection.	In the new proposed method, the under damped natural frequency ω_n is calculated via considering the t_{rise} from 10% to 90% of the overshoot.	[9]
2017	Development and analysis of GSM based gas leakage alerting system.	Successful wireless GSM aided alerting for possible fire accidents.	[10]
2017	Development of a wireless Electronic nose using artificial neural network for various gas concentration monitoring.	Artificial neural network had been used to estimate the concentration of a gas in the air based on the ratio.	[11]
2017	Internet of Things-based cargo monitoring system (IoT-CMS) to monitor any environmental changes.	Introduced WSN and Fuzzy Logic Control simultaneously for the first time.	[12]
2018	IoT based cold storage temperature and humidity monitoring.	Showed how to control actuators over the net by just changing the state wise parameters from “0” to “1” and vice versa for controlling.	[13]
2018	Smart irrigation controlling system by using IoT.	The data and control were hosted in an online IoT platform. The IoT platform provides real-time monitoring and control via a simplified online Graphical User Interface (GUI).	[14]

2. Project Planning & Algorithm

This project deals with monitoring LPG leakage along with administrative alert by giving buzzer sound, switching on specified relay(s) and sending an alert message to administrator(s) to decide about the precautional measures. For this purpose, gas leakage concentration is sensed by gas sensor (MQ-6) which sends the data (analog) to the controller (*NodeMCU*) where the analog value is subjected to a sequential conversion to predict the probable intensity of gas inside the control volume and on crossing a reference threshold value (set by administrator/operator) the controller it switches ‘ON’ the relay(s) and buzzer(s) alerting to the administrator/operator of the plant (Industry/Home) including an extra control-option through manual control utilizing the IoT server to prevent accidents from the leakage. Fig. 1 shows the flow chart of the experimental system and Fig. 2, Fig. 3 shows the schematic block diagram and the experimental setup of the system respectively.

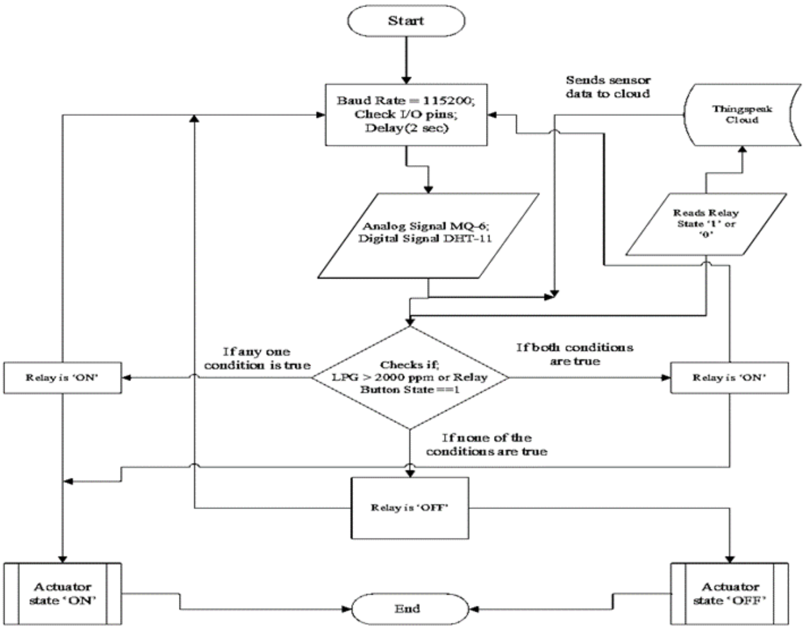

Fig. 1 Flowchart of the fabricated control system.

From the flowchart (Fig. 1), it is noticed that the controller sets its Baud Rate or Sampling Frequency, Check Input-Output Pins and the delay time/samples before starting sensory data-logging. Then the analog signal from gas sensor along with the digital signal from the relative humidity sensor is read and stored inside the read-only-memory of the controller for a specified timestamp constantly. The gas sensor data is subjected to ADC (Analog to Digital Conversion) followed by voltage measurement from which the sensed gas concentration level is calibrated by means of coding. Then a comparator (+/-) controls the feedback action and the wireless chip (ESP-8266) sends collected data to an authenticated server with an ISP (Internet Service Provided) activated router.

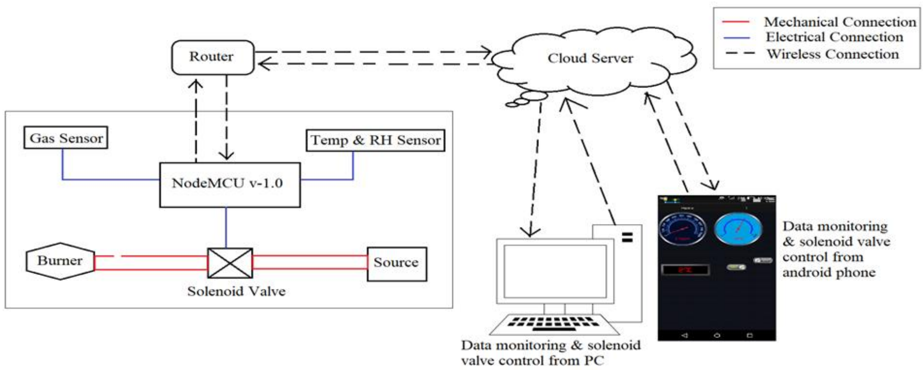

Fig. 2 System Setup (Schematic).

The system schematic shown in Fig. 2, is a graphical representation of the experimental system (Fig. 3). Here the NodeMCU used as controller is electrically connected to an analog sensor, a digital sensor and a high volt-amp rated actuator. The data transfer protocol used in this experiment is MQTT (Message Queuing Telemetry Transport); which is a low-space data transferring protocol widely used in wireless transmission.

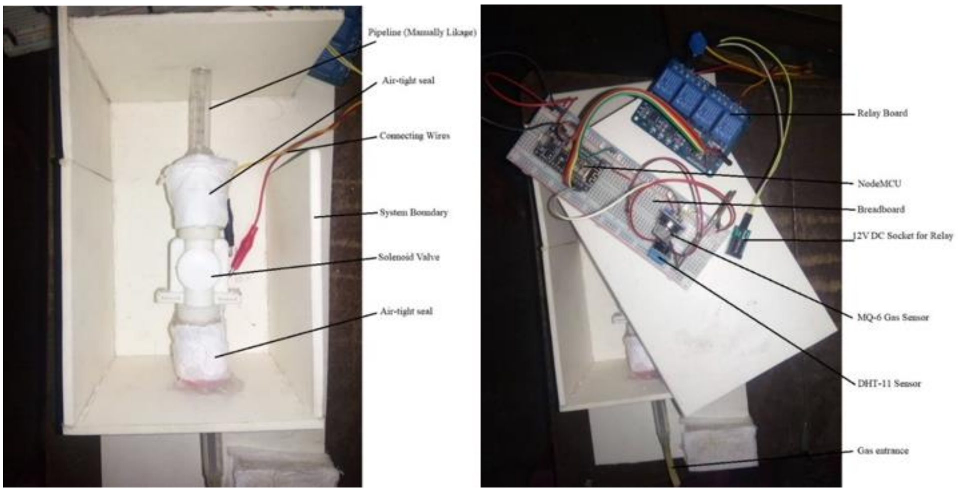

Fig. 3 Experimental Setup.

3. Mathematical Model for Gas Sensor Calibration

As the system focuses on gas concentration-based alerting and control of appliances, thus only MQ-6 gas sensor calibration (analog value to ppm) is considered for the mathematical analysis. DHT-11 sensor is to for checking the conditional Temperature and Relative Humidity as per gas sensor's datasheet. The gas sensor circuit schematic is shown in **Fig. 4**.

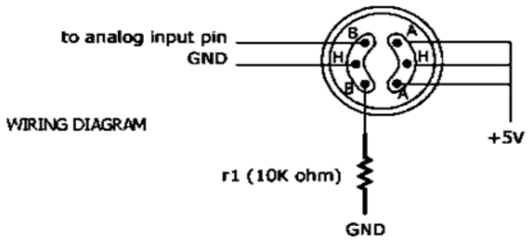

Fig. 4 MQ-6 gas sensor equivalent circuit schematic.

Let, V_C = Supply Voltage = +5V, R_S = Sensor Resistance, R_L = Load Resistance (Variable), V_{RL} = Sensor output Voltage. From, Current flow and Voltage relationship,

$$V = I \times R \tag{1}$$

Here, $V = V_c$ & $R = R_s + R_L$, so, equation-(1) becomes;

$$I = \frac{V_c}{R_S + R_L} \tag{2}$$

Again, from equation-(1);

$$V = I \times R; or, V_{RL} = [{}^{V_c}/_{(R_S + R_L)}] \times R_L = \frac{(V_c \times R_L)}{(R_S + R_L)} \tag{3}$$

From, equation-(3);

$$V_{RL} \times (R_s + R_L) = V_c \times R_L; or, R_s = [(V_c \times R_L)/V_{RL}] - R_L \tag{4}$$

Fresh air resistance ration for gas sensors: R_S/R_0 = 4.4 ppm (MQ-4), 9.8 (MQ-2), 10 (MQ-6) [23]. Now, for calibrating sensor data the equation of a straight line can be beneficial. From normal geometrical analysis, the basic equation of a straight line is;

$$y = mx + b \tag{5}$$

Here, y = value on Y-axis; x = value on X-axis; m = Slope of line; b = Intercept from Y-axis. For analyzing sensitivity from R_S/R_0 vs ppm graph (log-log plot) with respect to datasheet, equation-(5) can be equated as;

$$Log_{10}(y) = m * Log_{10}(x) + b \tag{6}$$

Slope (m) Value formula: If (x_0, y_0) and (x, y) are any two points of a line from a log-log plot then the formula for determining m is;

$$m = Log_{10}({}^{y}/_{y_0}) / Log_{10}({}^{x}/_{x_0}) \tag{7}$$

Intercept from Y-axis (b) is given in equation-(6);

$$Log_{10}(y) = m * Log_{10}(x) + b; or, b = Log_{10}(y) - m * log_{10}(x) \tag{8}$$

Using equations-(1) to (8) the gas concentration can be determined directly in ppm (Parts per millions): Gas concentration, $C = [Log_{10}(\frac{R_S}{R_0}) - b]/m$ in parts per million (ppm) unit. Where, R_S/R_0 = Gas sensor sensitiveness, b = Interception from Y-axis (From, Sensor Datasheet; Sensitiveness vs PPM Graph), Slope (m) $= -(dy/dx)$. From, the equations of analog signals of 1024 (2^{10}) resolutions; Gas Sensor's Sensitivity = R_{S0}/R_0. Where, R_{S0} = Sensor Output Resistance at experimental environment, R_0 = Sensor Output Resistance at ideal environment (1000 ppm of LPG, 25^0 C. & 60% RH). At 32^0 C. & 55-65% of RH environment; Sensor Sensitivity, R_{S0}/R_0 = 9.8 (in fresh air for MQ-6) [14]. In this study, at 27^0 C. & 67% of RH environment; Sensor Sensitivity, R_S/R_0 = 8.71 (at normal room condition) is obtained from ADC [14, 15].

4. Test Outputs & Signal Processing

From experimental data, various calculations were performed using 'MATLAB' environment. The Digital Signal Analysis-Toolbar is a great tool for signal processing and smoothing. As the data transfer took place using wireless media thus some additional noise was logged in an arbitrary manner. To overcome the problem a processing is needed. For this research, mainly Fast Fourier Transformation (FFT) was performed for better signal processing. The analysis procedure along with relative graphs are descried below;

Coherence Estimation via Welch Method: In digital signal processing, coherence is a statistics between two functions or signals which is used to estimate the power transfer of the input and output in a linear/linear time-invariant system. This algorithm is based on standard MATLAB's tools. The standard derivation of the mean is computed as [15-18];

$$\sigma(f) = \sqrt{2(1-|\Upsilon(f)|^2)^2/N|\Upsilon(f)^2|} \quad (9)$$

$$|\Upsilon(f)|^2 = \left|P_{xy}(f)\right|^2/(P_{xx}(f).P_{yy}(f)) \quad (10)$$

If, $x(t)$ and $y(t)$ are two real value time variant functions where the coherence between the two signals is termed as $\Upsilon(f)$ (sometimes also called magnitude squared coherence) and $\sigma(f)$ is the standard deviation of the mean. By using equations-(9) & (10), Fig. 5, is plotted where a normalized frequency is used for better visualization which depicts the coherence estimation via Welch method. The figure shows that no data has been overlapped into one another which verifies the continuous datalogging as quite satisfactory.

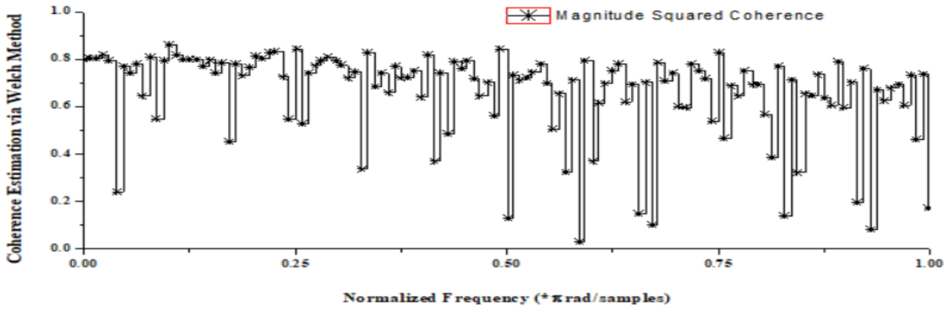

Fig. 5 Coherence estimation via Welch method.

The Fig. 6, denotes the magnitude response curve. The rms signal-to-noise ratio for an ideal N-bit converter is;

$$\text{SNR} = 20log_{10} * (r.m.s\ value\ of\ F_s\ input/r.m.s\ value\ of\ quantization\ noise) \quad (11)$$

or,

$$\text{SNR} = 20log_{10}\frac{q^{2^N}/2\sqrt{2}}{q/\sqrt{2}} = 20log_{10}2^N + 20log_{10}\sqrt{\frac{3}{2}} \quad (12)$$

SNR = 6.02N + 1.76 dB, over the Nyquist bandwidth of interest.

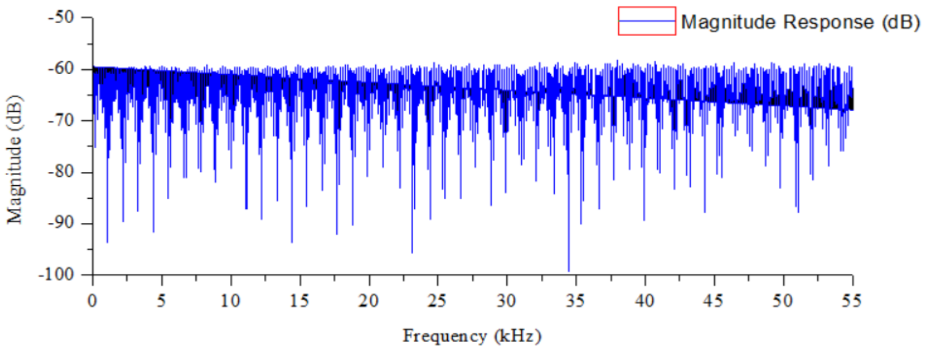

Fig. 6 Magnitude Response Graph (Gas Sensor).

Time-Domain signal processing: Now, using the gas sensor data Time-Domain graph was plotted in Fig. 7(a) to Fig. 7(d), along with a 3rd and 8th order Fast Fourier Transformation (FFT) of the signal for better analysis. This is achieved, in a process known as convolution, by fitting successive sub-sets of adjacent data points with a low-degree polynomial by the method of linear least squares [19]. Fig. 7(a) depicts the plots of Raw analog, Savitzky-Golay Filtered value, moving average filtered value and the median plot.

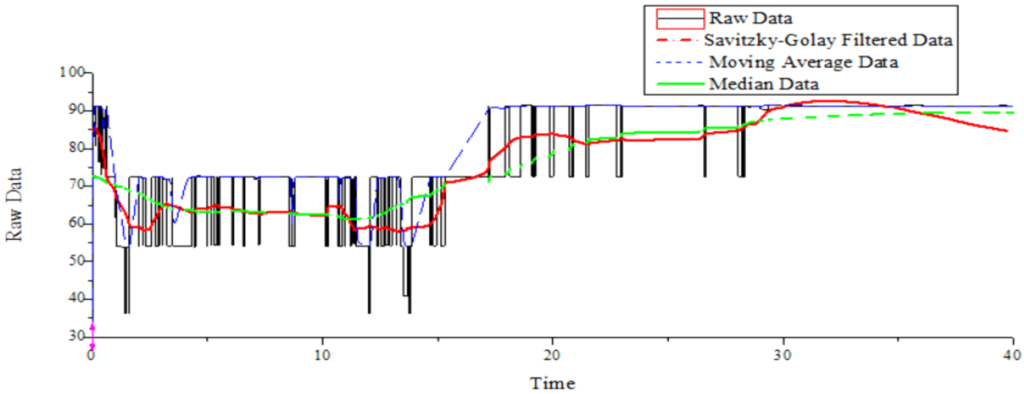

Fig. 7(a) Processed Signal (PPM vs Time).

Fig 7(b) shows the Furrier fitted curve for gas sensor value from which the best suited filter was found to be the 5th order FFT. The higher and lower range has also been showed along with residuals plotted in black color. This signal filtration was done under room environment with no manual gas leak. By comparing the plots of Fig. 7, the 5th order FFT was finally considered as the filter for signal processing having very low range of residuals.

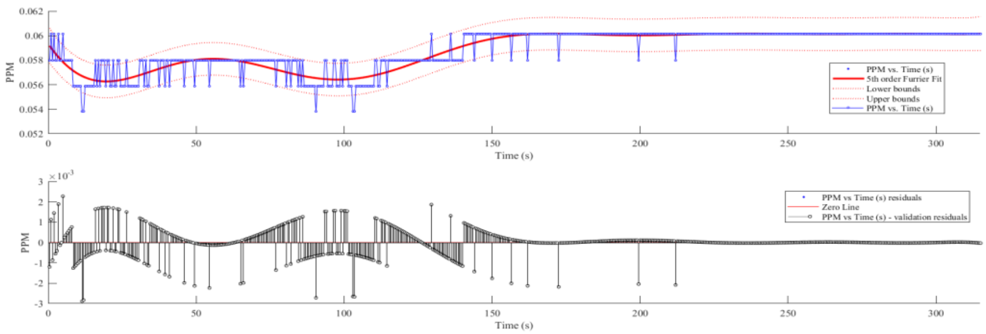

Fig. 7(c) PPM vs Time Domain. (5th order FFT with 95% confidence limit).

The below Fig. 7(c) & (d) are the same plots as Fig. 7(a) & (b), but those value represents the Temperature and Humidity. The same method of simulation was considered for both sensor's data smoothing with respect to time.

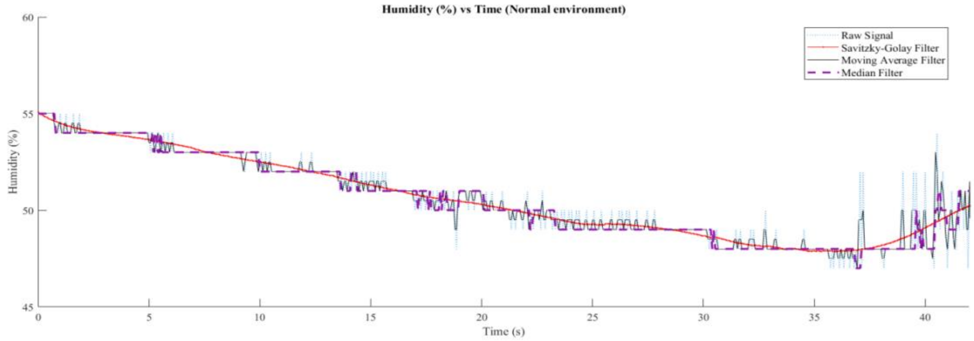

Fig. 7(c) Processed Signal (Humidity vs Time).

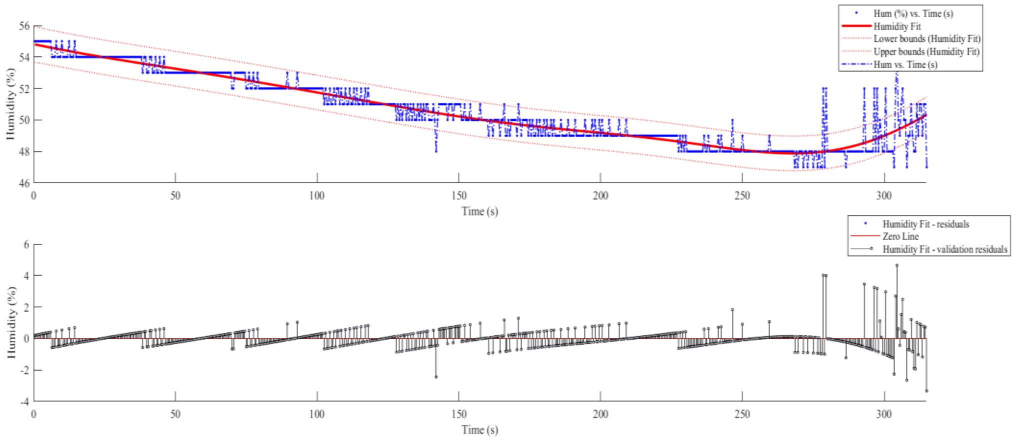

Fig. 7(d) Humidity vs Time domain graph (8th order FFT of 95%).

Group delay response analysis: Now from convolution theorem, if y is a time-variant function of x ($y = F(x,t)$) and the function x is in a convoluted form with some other similar time-variant function h then [20-24],

$$y(t) = (h * x)(t) \stackrel{\text{def}}{=} \int_{-inf.}^{+inf.} x(u)h(t-u)du \tag{13}$$

In signal processing, $y(t)$ dependent mostly on the subsequent values of x that occurred near the time t. So, for any linear system;

$$O_t\left\{\int_{-inf.}^{+inf.} c_\tau . x_\tau(u)d\tau;\ u\right\} = \int_{-inf.}^{+inf.} c_\tau . y_\tau(t)d\tau;\ u \tag{17}$$

and the time-invariance requirement is;

$$O_t\{x(u-\tau); u\} = y(t-\tau) \stackrel{\text{def}}{=} O_{t-\tau}\{x\} \tag{18}$$

From, eqn-13 to 18, the impulse response can be noted as;

$$h(t) \stackrel{\text{def}}{=} O_t\{\delta u;\ u\} \tag{19}$$

From, equations-(12) to (19), using Amplitude sampling technique; Fig. 7(e) to Fig. 7(k) are be computed numerically along with related graphical representation. Fig. 7(e) is the group delay response plot for the gas sensor which shows that between 11.3-12.2 kHz of sampling frequency the delay remains constant. Fig. 7(f) represents the phase delay (with respect to samples), which shows positive noise addition in the cloud data thus a low-pass filter should be mounted with the sensor's input pin in series resulting in about 80-85% reduction of induced noise.

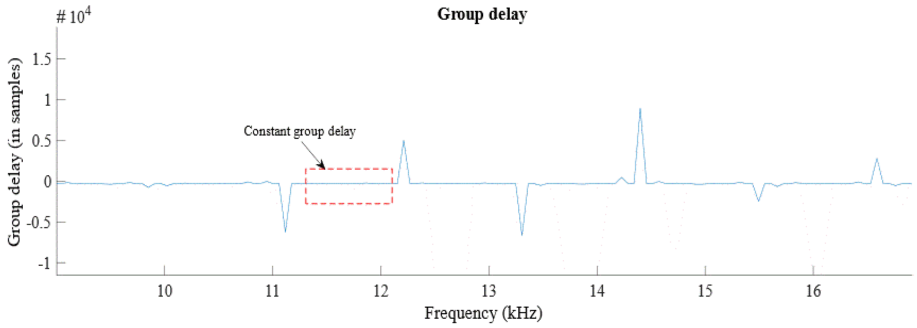

Fig.7(e) Group Delay Response.

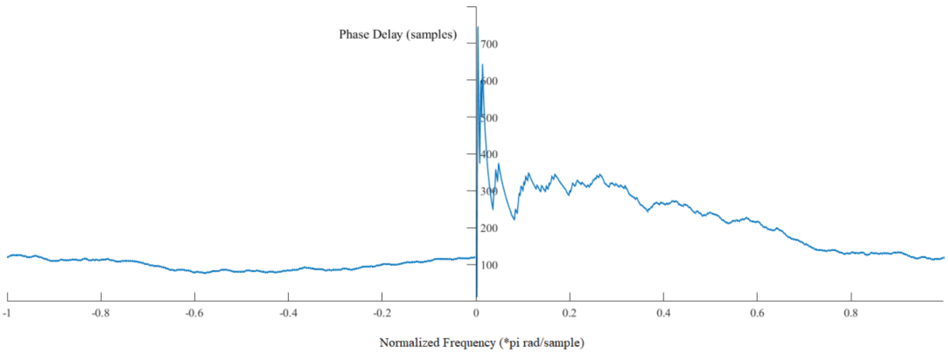

Fig. 7(f) Phase Delay Samples.

Fig. 7(g), denotes the pole-zero plot for the system, which shows that this system has some noise but ultimately it is stable. To make datalogging more stable, the phase delay response should be reduced to almost zero value, which is induced mainly because of using an old and very low-cost sensor. It can be reduced by using a low pass filter (as it controls the positive phase delay addition) at the input or by using sensors from renowned brands.

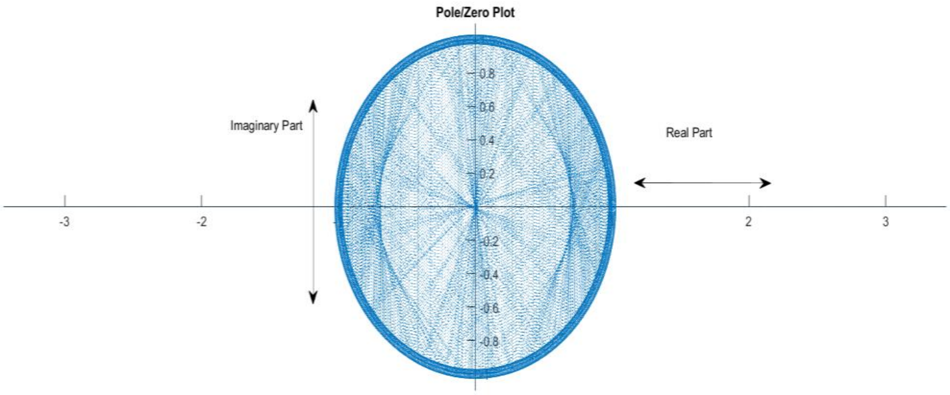

Fig. 7(g) Pole Zero Plot.

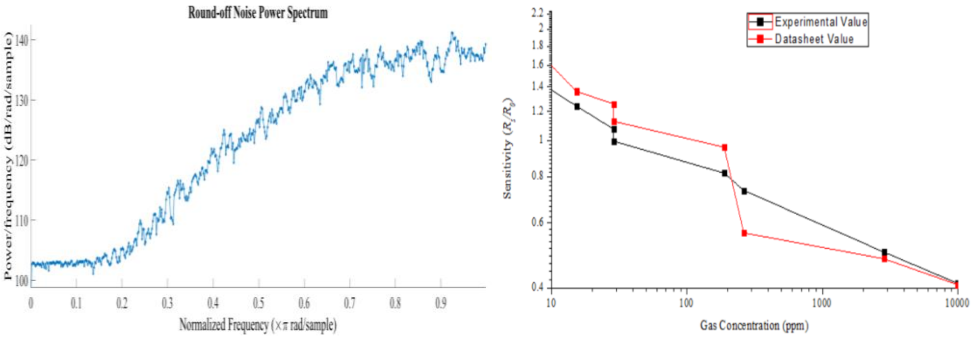

Fig. 7(h) Power Spectrum (**L**) and Sensitivity vs ppm plot (**R**).

Fig. 7(h) is the round-off noise power spectrum plot for the system showing the power band of the induced noise due to positive phase addition and also shows the actual & experimental Sensitivity vs Concentration plot, from where it can be said that the calibration was 90-95% accurate, which is good.

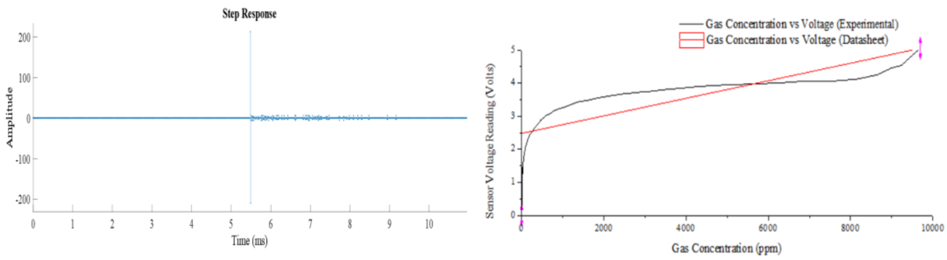

Fig. 7(i) Step response (**L**) and ppm vs Voltage plot (**R**).

From, Fig. 7(i), the step response (Left) can be shown where it is seen that initially the system runs fine but after a certain period it shows some abruptions but the statistical filter automatically fixes the errors resulting in a smooth response. It also shows the experimental and simulated relationship between supplied voltage and gas concentration. The below, Fig. 7(j) shows the time domain and frequency domain analysis plot for the system showing initial sensory noise. The transfer function of the system can be estimated by using Welch Transfer function distribution theory, which is plotted on Fig. 7(k).

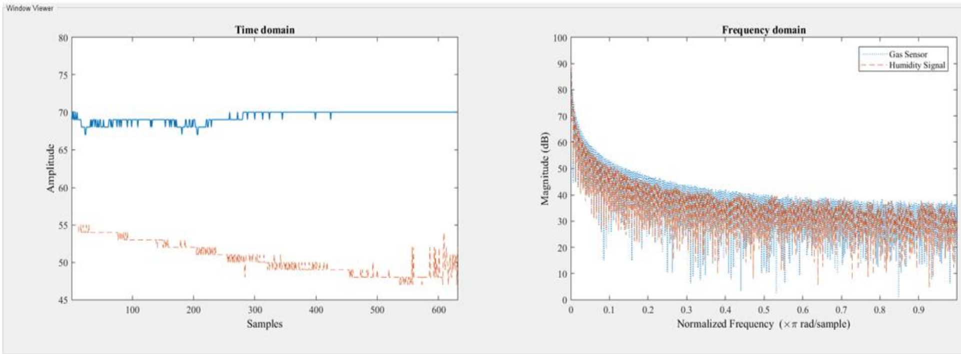

Fig. 7(j) Time domain and Frequency domain graph for the system.

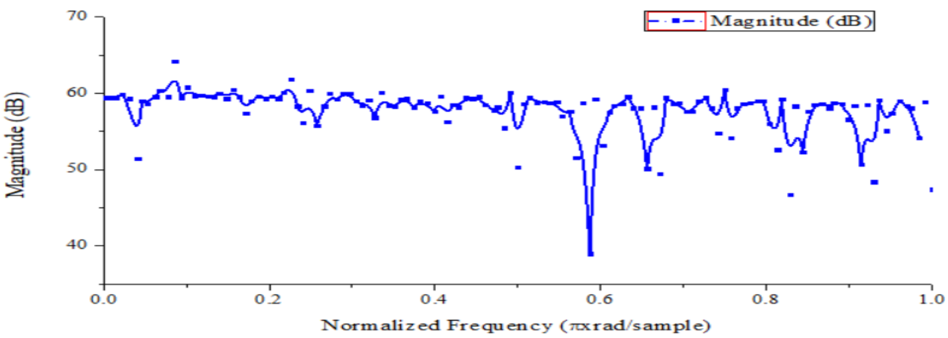

Fig. 7(k) Transfer function estimation via Welch distribution.

5. DESIGN OF CONTROL SYSTEM

Feedback and Feedforward both control options were applied to the experimental prototype. Combining these two control options is the most challenging part for this research. The experimental threshold for gas sensor was set 300 ppm. For the feedback control, when the nearby gas concentration crosses 300 ppm then the controller automatically will set the actuator off for a certain delay period and rechecks the value of sensor again and again. If the value goes below 300 ppm then again for a certain period the actuators are turned on by a digital signal, but if again the gas concentration crosses 300 ppm then the system detects a gas leakage problem and the source valve is turned off.

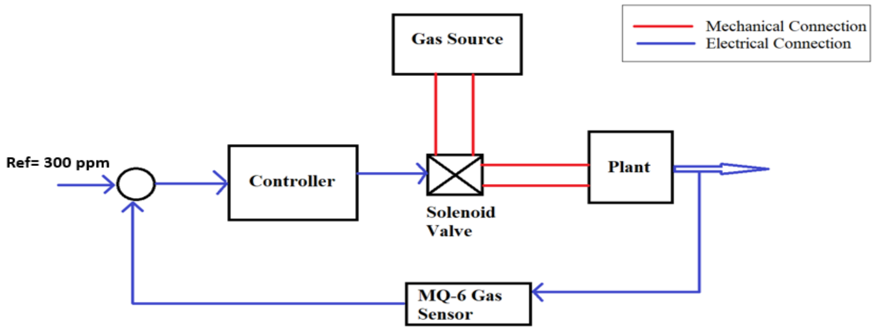

Fig. 8(a) Feedback control for proposed system.

Fig. 8(a), shows the schematic of the developed feedback control system of the experimental system. In this device, the mean error will be the mathematical summation of Desired voltage and measured voltage and those two voltages are different in terms of signs. The desired value will be always positive, and the measured value is always negative. So, when those two values are equal but opposite in signs, so there will be no errors in the control system and that will be an absolute equilibrium condition [25-27]. Thus, this type of feedback control system is very effective to use.

Feedforward control in simple terms mean controlling something by the aid of a manual signal. In this research, when feedback control crashes or manual switching is needed then from the server a predefined signal is sent to the controller and selected actuators can be controlled. Fig. 8(b) shows the schematic of the applied feedforward mechanism for controlling actuators using manual command over IoT.

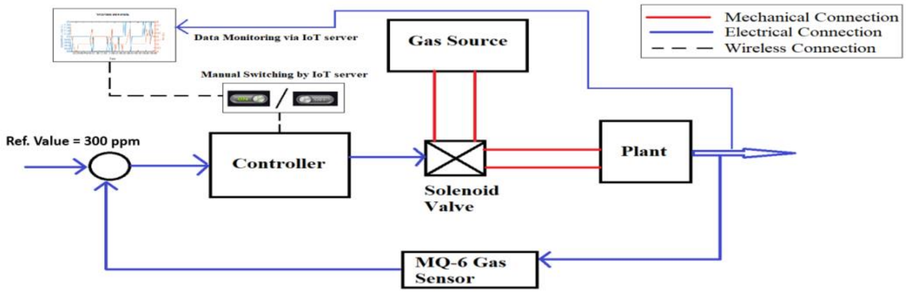

Fig. 8(b) Feedforward control system for the experimental setup.

The feedforward controlling actions is implemented using ‘https-request’ protocol used for single way communication. The control algorithm for this research has been formulated through some logical reasonings followed by C^{++} code maintaining the fuzzy logics given in Table 2.

From the Fuzzy logics, nine probabilities of actuation is possible by generating C^{++} code upon those logics, where two variables namely ‘https-request’ (Feedforward command - 1 or 0, if undefined, set value = = 0) and ‘Gas concentration’ (Reference value- <300 = = 0, >300 = = 1, if value = 300, set value = = 0) are liable to specified controller responses followed by series change in actuation commands from controller utilizing both feedback and feedforward control actions simultaneously.

Table 2 Control Logics topology for proposed system.

	'https-request' from server (Str.)	Gas Concentration (ppm)	Controller response (Bin)	Actuator output (Bin)
Logic-1	0	<300	0	0
Logic-2	0	>300	1	1
Logic-3	1	>300	1	1
Logic-4	1	<300	1	1
Logic-5	Undefined (= = 0)	<300	0	0
Logic-6	Undefined (= = 0)	>300	1	1
Logic-7	0	=300	0	0
Logic-8	1	=300	1	1
Logic-9	R	0	Reset	1

6. SYSTEM PERFORMANCE ANALYSIS

To make a system performance analysis total 20 trials have been made. The trials were successfully investigated, and no major error was observed. The below Table 3 shows the performance test results. In this investigation, the commands were performed using the cloud-server followed by observation in actuation using the experimental setup described earlier in Fig. 3 by the mobile application. Fig. 9 represents the system performance test outputs in a graphical manner.

Table 3 System performance data table.

No of Obs.	Gas Concentration	HTTPS Input	Actuator Response	Elapsed Time (sec)	Experimentation
1	170 (= = 0)	0	0	0 (start)	Success
2	173 (= = 0)	1	1	15.3	Success
3	211 (= = 0)	0	0	20	Success
4	288 (= = 0)	1	1	11	Success
5	316 (= = 1)	0	1	7.5	Success
6	375 (= = 1)	1	1	N/A	No Specified Change
7	402 (= = 1)	0	1	N/A	No Specified Change
8	287 (= = 0)	1	1	12	Success
9	255 (= = 0)	1	1	N/A	No Specified Change
10	221 (= = 0)	0	0	15.7	Success
11	300 (= = 0)	0	0	N/A	No Specified Change
12	300 (= = 0)	1	1	13.4	Success
13	302 (= = 1)	2	1	Error	Error
14	380 (= = 1)	4	1	Error	Error
15	293 (= = 0)	0	0	12	Success
16	319 (= = 1)	R	Reset	N/A	Reset of process
17	327 (= = 1)	1	1	18	Success
18	289 (= = 0)	0	0	8	Success
19	294 (= = 0)	1	1	11	Success
20	277 (= = 0)	0	0	5	Success

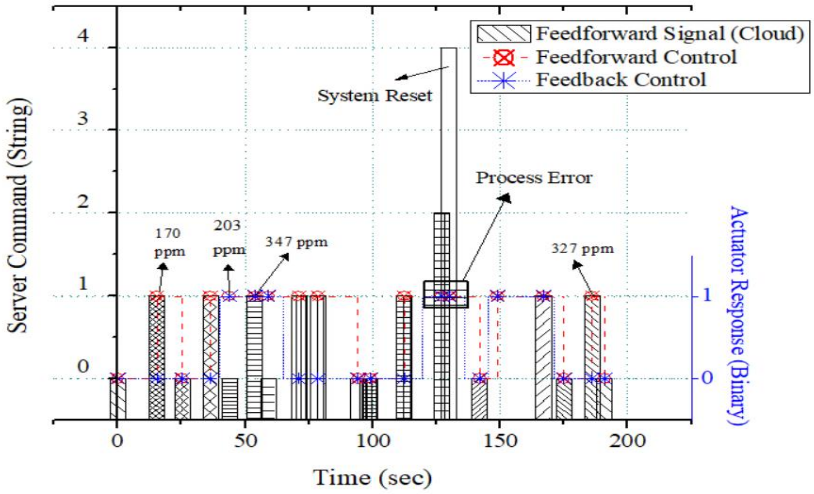

Fig. 9 Feedback and Feedforward control from system performance test.

All the evaluation shows that the total system behaves like an error free system. Though the data processing time is a bit long (avg. 13 sec.) but the system behavior seemed better. This system processing delay can be optimized by using manual api and custom server. As *Thingspeak* gives free access to students limiting browsing speed; so, no one can misuse it for commercial purpose. The below Fig. 10 shows the graphical states of those experimental setup. This fabricated system can be used to prevent

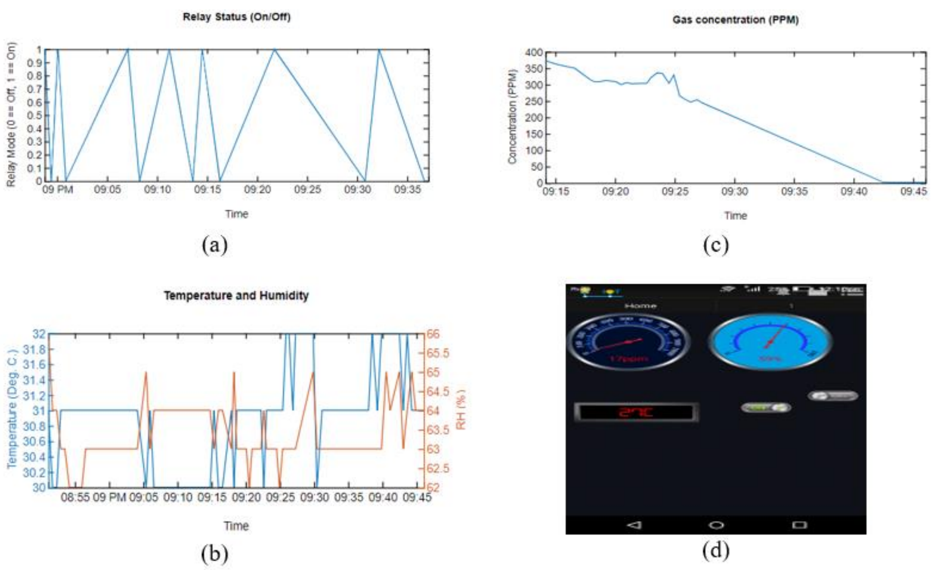

Fig. 10 Graphical presentation of monitored data; (a) Relay state data; (b) Temperature and RH data; (c) ppm Concentration of LPG gas and (d) Android application GUI.

accidents caused by gas leakage in home and industrials. In process, food, chemical and fertilizer industries various types of toxic-hydrocarbon based gases (may have ability to ignite fire) are used widely thus making the industries more viable to accidents due to unnoticed leakage of those gases. The fabricated prototype has almost 95% efficiency along with both feedback and feedforward control options which makes it more stable to monitor and prevent unnoticed gas leakage crossing a defined reference value. The implemented cloud server controlling (feedforward) actions prove the system's infinite (very long range) distance actuating capability but it is very necessary to get connected with ISP for both controllers (Transmitter and Receiver).

6. System Performance Analysis

The fabricated system run successfully, and 20 trials were performed to measure its performance. It showed no errors in those 20 trials which took almost 3 hours to execute. The control system took almost 13 seconds to perform necessary commands when signals came from the host server. This delay period can be overcome by using the premium version of *Thingspeak* server. This delay period can be shortened up to 4 seconds as it is the minimal period of IoT server refreshing. It is apparent from analyzed signals that the impulse response and the group delay response are seemed quite perfect if the Baud Rate (Sampling Frequency) tuning ranges from 11 to 12.6 kHz. In this study, 11.52 kHz Sampling Frequency is used. The power density spectrum of gas sensor is quite fine although the Signal to Noise ratio is comparatively higher. This can be overcome by using a 20-pF ceramic disk capacitor as it can work as a low pass filter. The overall system efficiency was about 95%, which is quite good for a robust controlling operation.

Acknowledgement: *The authors gratefully acknowledge the financial support received from the University Grant Commission (UGC), Bangladesh. The authors thank Mr. S. M. Asif Hossain (Dept. of Electronics and Communication Engineering, KUET) and Md. Robiul Islam (Lecturer, Dept. of Mechatronics Engineering, RUET) for their contributions in this study.*

References

[1] J. Wang, M. Tong, X. Wang, Y. Ma, D. Liu, J. Wu, D. Gao & G. Du, "Preparation of H2 and LPG gas sensor", *Sensors and Actuators B: Chemical*, vol. 84, no. 2-3, 95–97, 2002.

[2] M. Miftakul Amin, M. Azel Aji Nugratama, Andino Maseleno, Miftachul Huda, and Kamarul Azmi Jasmi. "Design of cigarette disposal blower and automatic freshner using mq-5 sensor based on atmega 8535 microcontroller." *International Journal of Engineering & Technology*, vol. 7, no. 3, pp. 1108–1113, 2018.

[3] N. Sinha, K. Eswari Pujitha, and J. Sahaya Rani Alex, "Xively based sensing and monitoring system for IoT", In Proceedings of the IEEE International Conference on Computer Communication and Informatics (ICCCI), 2015, pp. 1–6, 2015.

[4] A. Mallik, S. A. Hossain, A. B. Karim, & S. M. Hasan, "Development of LOCAL-IP based Environmental Condition Monitoring using Wireless Sensor Network", *International Journal of Sensors, Wireless Communications and Control*, vol. 9, pp. 1–8, 2019.

[5] K. Keshamoni, and S. Hemanth. "Smart Gas Level Monitoring, Booking & Gas Leakage Detector over IoT", In Proceedings of the 2017 IEEE 7th International Advance Computing Conference (IACC), pp. 330-332. 2017.

[6] A. Mallik, A. Ahsan, M. M. Z. Shahadat and J. C. Tsou. "Man-in-the-middle-attack: Understanding in simple words." Int. J. Data Networks and Security, (2019)

[7] V. Yadav, A. Shukla, S. Bandra, V. Kumar, U. Ansari, and S. Khanna. "A Review On Iot Based Hazardous Gas Leakage Detection & Controlling System Using Microcontroller & Gsm Module." *Journal of VLSI Design and Signal Processing*, vol. 3, no. 1, 2017.

[8] M. Sharma, D. Tripathi, N. P. Yadav, and P. Rastogi, "Gas Leakage Detection and Prevention Kit Provision with IoT." *Gas,* vol. 5, no. 02, 2018.

[9] A. J. Moshayedi, M. V. Kukade, and D. Gharpure, "Electronic-nose (E-nose) for recognition of Cardamom, Nutmeg and Clove oil odor", 2014.

[10] V. V. Alekseev, V. S. Konovalova, and E. N. Sedunova, "Information-measurement and control system “smart house” as object of practice-oriented training of master's degree “instrumentation technology”", In Proceedings of the International Conference "Quality Management, Transport and Information Security, Information Technologies"(IT&QM&IS), 2017, pp. 612–615.

[11] S. I. Sabilla, R. Sarno, and J. Siswantoro. "Estimating gas concentration using artificial neural network for electronic nose", *Procedia Computer Science,* vol. 124, pp. 181–188, 2017.

[12] Y. P. Tsang, K. L. Choy, C. H. Wu, G. T. S. Ho, H. Y. Lam, and P. S. Koo. "An IoT-based cargo monitoring system for enhancing operational effectiveness under a cold chain environment." *International Journal of Engineering Business Management*, vol. 9, 1847979017749063, 2017.

[13] A. B. Karim, A. Z. Hassan, and M. M. Akanda. "Monitoring food storage humidity and temperature data using IoT." *MOJ Food Process Technol,* vol. 6, no. 4, pp. 400–404, 2018.

[14] J. Mari, J. Maja, J. Robbins, "Controlling irrigation in a container nursery using IoT", *AIMS Agriculture and Food*, vol. 3, no. 3, pp. 205–215, 2018.

[15] A. Brandt, "A signal processing framework for operational modal analysis in time and frequency domain", *Mechanical Systems and Signal Processing,* vol. 115, pp. 380–393, 2019.

[16] S. A. Hossain, M. Hossen, and S. Anower, "Estimation of damselfish biomass using an acoustic signal processing technique", *Journal of Ocean Technology*, vol. 13, no. 2, 2018.

[17] S. Mariani, L. Tarokh, I. Djonlagic, B. E. Cade, M. G. Morrical, K. Yaffe, K. L. Stone et al, "Evaluation of an automated pipeline for large-scale EEG spectral analysis: the National Sleep Research Resource", *Sleep medicine,* vol. 47, pp. 126–136, 2018.

[18] TNS Tengku Zawawi, A. R. Abdullah, W. T. Jin, R. Sudirman, and N. M. Saad, "Electromyography Signal Analysis Using Time and Frequency Domain for Health Screening System Task", *International Journal of Human and Technology Interaction (IJHaTI),* vol. 2, no. 1, pp. 35–44, 2018.

[19] S. A. Hossain, M. Hossen, A. Mallik, and S. Mahmudul Hasan, "A Technical Review on Fish Population Estimation Techniques: Non-Acoustic and Acoustic Approaches." *Akustika*, vol. 31, pp. 87–103, 2019.

[20] Regalia, Phillip. *Adaptive IIR filtering in signal processing and control*. Routledge, 2018.

[21] B. Boashash, A. Aïssa-El-Bey, and M. F. Al-Sa’d. "Multisensor Time–Frequency Signal Processing MATLAB package: An analysis tool for multichannel non-stationary data", *SoftwareX*, 2018.

[22] A. E. Cohen, "Automated HDL signal processing deployment performance from high level MATLAB specification for an unmanned aerial vehicle (UAV)", In Proceedings of the *IEEE 8th Annual Computing and Communication Workshop and Conference (CCWC), 2018*, pp. 900-905. IEEE, 2018.

[23] Van Drongelen, Wim. *Signal processing for neuroscientists*. Academic press, 2018.

[24] S. A. Hossain, A. Mallik, and Md Arefin, "A signal processing approach to estimate underwater network cardinalities with lower complexity", *Journal of Electrical and Computer Engineering Innovations,* vol. 5, no. 2, pp. 131–138, 2017.

[25] U. Yilmaz, A. Kircay, and S. Borekci, "PV system fuzzy logic MPPT method and PI control as a charge controller", *Renewable and Sustainable Energy Reviews,* vol. 81, pp. 994–1001, 2018.

[26] W. He, T. Meng, D. Huang, and X. Li, "Adaptive boundary iterative learning control for an Euler–Bernoulli beam system with input constraint", *IEEE transactions on neural networks and learning systems,* vol. 29, no. 5, pp. 1539–1549, 2018.

[27] Steven Walczak, "Artificial neural networks." In *Advanced Methodologies and Technologies in Artificial Intelligence, Computer Simulation, and Human-Computer Interaction*, pp. 40-53. IGI Global, 2019.